한국지반공학회논문집 제23권 1호 2007년 1월 pp. 13 ~ 21

Rock Socket Roughness with Drilling Tools

굴착장비에 따른 암반근입말뚝의 공벽 거칠기

Moon S. Nam[1] 남 문 석

요 지

암반에 근입된 현장타설말뚝은 뛰어난 암반의 지지능력을 이용함으로써 교량이나 다른 대형구조물의 기초형식으로 널리 사용 중이다. 이러한 암반 근입 말뚝의 지지력은 주면 마찰력과 선단지지력으로 나누어 지는데, 이 중 암반부의 주면마찰력이 대부분의 상부하중을 지지하는 경우가 많다. 몇몇의 연구자들에 의하여 암반 근입부의 공벽 거칠기가 주면마찰력에 영향을 준다는 보고를 하였으나, 거칠기에 중요한 영향을 미칠 것으로 판단되는 굴착장비에 따른 거칠기에 관한 연구는 부족한 실정이다. 본 연구에서는 현장시험을 통하여 암반 굴착장비에 따른 공벽 거칠기에 대한 영향을 분석하였고, 그 결과로 굴착도구가 거칠기에 영향을 미치는 것으로 확인되었다.

Abstract

Rock socketed drilled shafts are used as foundations for bridges and other transportation structures because of their load carrying capabilities. However, only limited information is available in the literature on the effects of roughness on the unit side resistance of rock socketed drilled shafts. The objective of this study is to investigate the effect of drilling tools on the socket roughness in soft clay shale in Texas. Field study showed that the drilling tools, auger and core barrel, produced different roughness in the boreholes.

Keywords : Drilling tools, Rock socketed drilled shafts, Roughness, Side resistance

1. Introduction

The demand for carrying higher loads coupled with the geological conditions has resulted in placing the drilled shafts in rocks. Rock socketed drilled shafts are increasingly used as foundations for bridges and other structures.

Numerous design methods for rock sockets have been developed throughout the world. Most of these methods use unconfined compressive strength (q_u) as a measure of rock capacity. Only a few studies have considered socket roughness along the sides of the socket in any explicit. The objective of this study is to quantify the effect of drilling tools on the roughness in the soft clay shale in Texas.

2. Design Method Considering Socket Roughness

Several models, including those of Horvath et al. (1983), Rowe and Armitage (1987), Kulhawy and Phoon (1993), O'Neill and Hassan (1993), and Seidel and Collingwood (2001) appear appropriate for developing relations between q_u and maximum unit side resistance (f_{max}) for soft rock sockets.

Seidel and Collingwood (2001) performed a parametric

1 Member, Senior Researcher, Dept. of Geotechnical Engrg., Highway & Transportation Technology Institute, Korea Highway Corp., msnam@freeway.co.kr

* 본 논문에 대한 토의를 원하는 회원은 2007년 7월 31일까지 그 내용을 학회로 보내주시기 바랍니다. 저자의 검토 내용과 함께 논문집에 게재하여 드립니다.

study using ROCKET, a model for predicting the shearing resistance of the side of a rock socket using a simulation program developed at Monash University, in Australia, sufficient to define a method for producing socket side shear-displacement relationship to assist designers to compute load-settlement behavior without rigorous numerical analyses. They proposed a shaft resistance coefficient (SRC), and it was represented as follows (Seidel and Collingwood, 2001).

$$SRC = \eta_c \frac{n}{(1+\nu)} \frac{\Delta r_e}{D_s}, \quad (1)$$

$$\Delta r_e = \frac{D_s (1+\nu) SRC}{\eta_c n}, \quad (2)$$

where η_c = construction method reduction factor, equal to 1 for socket with clean unbonded concrete-rock interface but possibly less than 1 for sockets with smear or residual mudcake from mineral drilling muds,

ν = Poisson's ratio of the surrounding rock,

n = ratio of rock mass modulus to unconfined compressive strength of the rock (E_m/q_u),

Δr_e = effective asperity roughness height, and

D_s = socket diameter.

Using a data base of rock-socket load tests, Seidel and Collingwood (2001) developed relationships between back-calculated values of Δr_e and q_u, and the results are shown in Figure 1. The results in Figure 1 contained many types of rock, including shale, mudstone, sandstone, schist, chalk and limestone. Specific results, however, are not identified according to rock type. Drilling tools, and their effect on socket roughness, likewise were not identified. Also, other models, including those of Horvath et al. (1983), Rowe and Armitage (1987), Kulhawy and Phoon (1993), and O'Neill and Hassan (1993) are not specific about rock type and drilling tools.

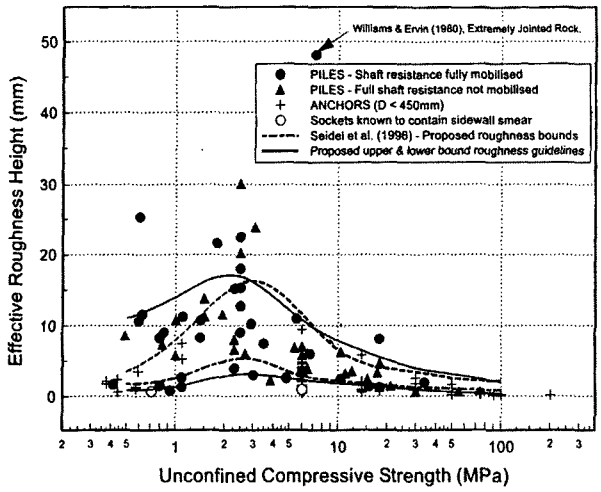

Fig. 1. Back-calculated values of Δr_e (Seidel and Collingwood, 2001)

3. Borehole Roughness Profile Device

A laser borehole roughness profile device (LBRP) was developed during this study in order to be adapted with the Kelly bar of a drill rig. The LBRP was based on the laser triangulation principle to measure the roughness. The hardware included a laser generator, a position sensitive device (PSD) as laser detector, signal processing circuits, laser control circuits, data acquisition, and digital control units. A block diagram of the hardware is shown in Figure 2 (Liang, 2002).

In order to measure the borehole roughness, the laser device was attached to the Kelly bar and lowered into the borehole to measure the roughness. A distance measurement device was attached to the Kelly bar to record the vertical distance. The LBRP measured the roughness at a speed of 100-kilo samples per second while the Kelly bar

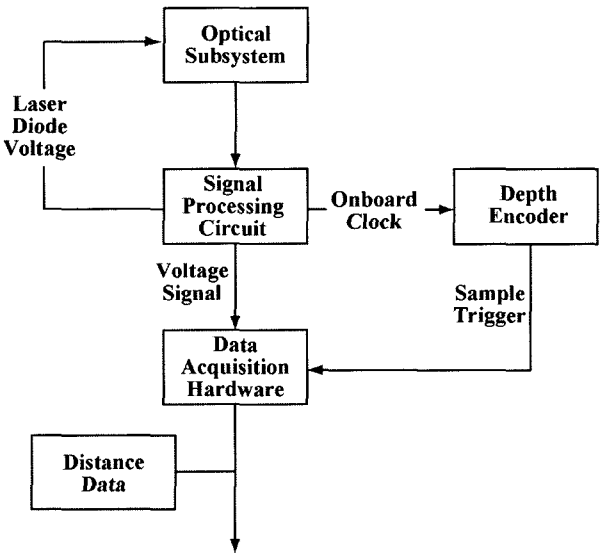

Fig. 2. Overall schematic of laser borehole roughness profiling system (Liang, 2002)

moved up from the bottom of the borehole (Figure 3). Four vertical profilings were measured, 90 degrees apart, at 6, 9, 12, and 3 o'clock positions in the borehole (Figure 3). The roughness measurement accuracy was better than 0.5 mm in both the vertical and radial directions (Liang, 2002).

The important part of the LBRP system is the laser device shown in Figure 3, which is based on the laser triangulation principle. The laser device consists of three parts: a laser diode module, convex lens, and a position sensitive detector (PSD). Figure 4 shows the laser triangulation distance measurement device. The laser diode module emits a laser beam to produce a light spot on a diffusive surface, and then the convex lens collects part of the reflected light and converges it to an image spot on the PSD. If the distance between the measurement device and the object surface changes, the position of image spot on the PSD will also be shifted. According to the position and the light intensity of the image spot, the PSD can output current signals to the electronic circuit. This is the basic principle of the laser triangulation distance measurement device as shown in Figure 5. Also, Figure 5 shows detail mathematical formulae used in determining the roughness height.

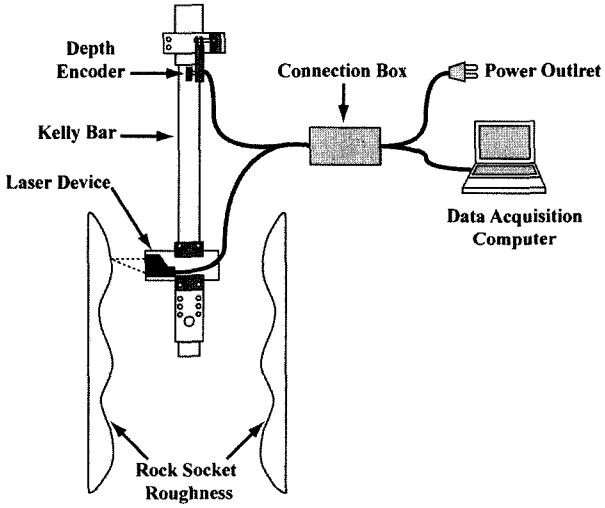

Fig. 3. Physical arrangement of LBRP system (Liang, 2002)

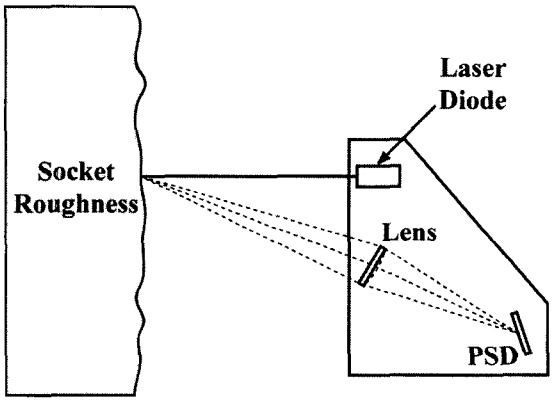

Fig. 4. Laser triangulation distance measurement device (Liang, 2002)

4. Construction of Test Sockets and Roughness Measurements

In order to investigate the effect of drilling tools on socket roughness, four test sites [Hampton (HT), Denton Tap (DT), Rowlett Creek (RC), and Texas Shafts (TS)] were selected in North Central Texas where soft rock formations are upper Cretaceous formations, including the Eagle Ford (clay shale) and Austin (limestone) formations. The test sites consisted of two clay shale sites (HT and DT) and two limestone site (RC and TS).

Two common types of rock drilling tools were used at the test sites: (1) an auger and (2) a core barrel to

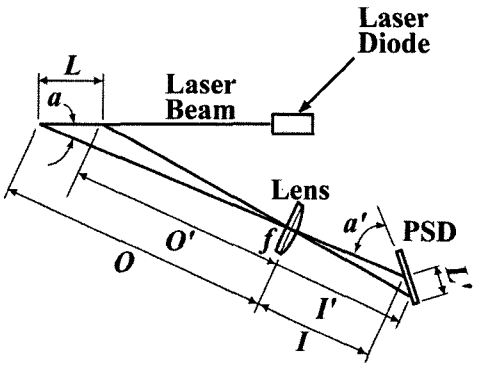

Basic Optics:

$$L=\frac{(O-f)L\sin a}{L\cos a\sin a+f\sin a}$$

$$\tan a'=\frac{L\sin a}{I-I'}=\frac{fL\sin a}{O-L\cos a-f}\times\frac{(O-f)(O-L\cos a-f)}{f^2L\cos a'}$$

$$I=\frac{Of}{O-f}\quad\text{and}\quad I'=\frac{f(O-L\cos a)}{O-L\cos a-f}$$

L' is sensed on the position sensitive detector (PSD); f is the known focal length of the lens, a (angle) is a designed property of the profiler (constant); the above three equations are solved simultaneously using software in the data acquisition system to obtain L.

Fig. 5. Principle of operation of laser borehole roughness profiling (Liang, 2002)

quantify borehole roughness. The auger was 724 mm in diameter and 1674 mm in height with heavy blunt flat blade teeth on double cutting edges and double flights. Outside tooth was turned slightly to the outside perhaps to give slightly larger outer diameter than 724 mm as shown in Figure 6 (a). The single-walled core barrel (CB-3610) had a diameter of 762 mm and height of 1270 mm with slightly out-sided heavy blunt conical teeth on the bottom of the single wall as shown in Figure 6 (b). Two boreholes were drilled in close proximity at the site.

Each borehole was profiled at 6, 9, 12, and 3 o'clock positions using the laser borehole profiling system as described before. The borehole roughness profile at each profile line was measured at 0.25 mm intervals (vertical distance), and all roughness profiles at each site are shown in Figures 7 to 10. Occasional spurious signals as very sharp spikes of very short wave length were filtered out of the data set. It must be noted that roughness profiles shown in these figures are referred to an arbitrary zero radius. That is, these profiles were not an indication of true borehole diameter.

Side view　　Bottom view

(a) Auger (Diameter of 724 mm and height of 1674 mm)

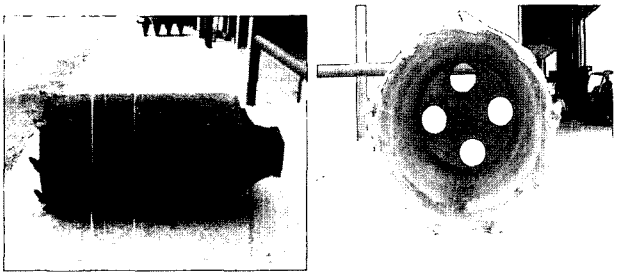

Side view　　Bottom view

(b) Core Barrel (Diameter of 762 mm and height of 1270 mm)

Fig. 6. Drilling tools

Graphically based on roughness profiles as shown in Figures 7 to 10, it was revealed that the type of drilling tools had significant effect on the borehole roughness. That is, the borehole roughness of core barrel test hole was consistently and relatively rougher than the auger test hole for all sites. Actual photos of boreholes at Texas Shafts' site, as shown in Figure 10, reinforce that the auger test hole was smoother than the core barrel test hole. This phenomenon may be caused due to the following reasons: (1) flat blade teethes of the auger resulted in smoother borehole than conical teethes of the

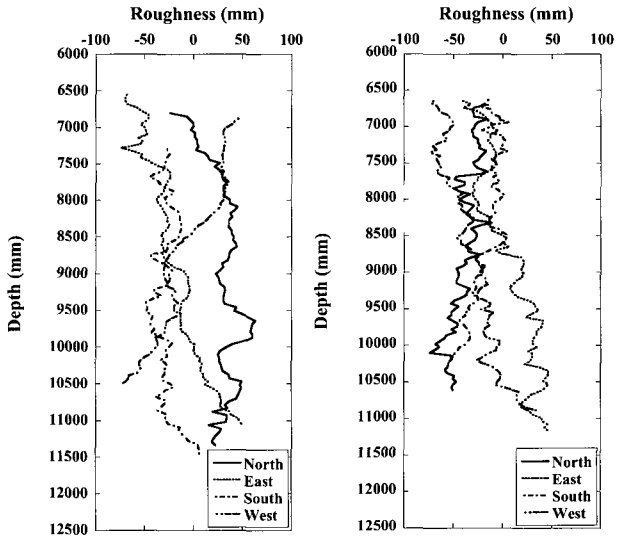

(a) Roughness by auger　　(b) Roughness by core barrel

Fig. 7. Roughness profiles at HT site

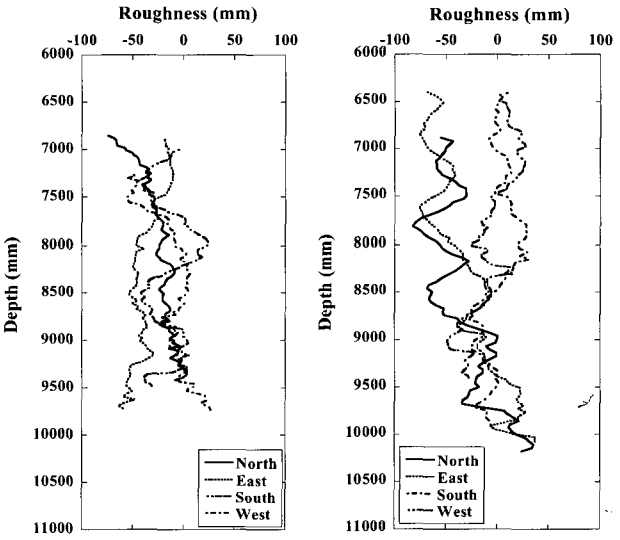

(a) Roughness by auger　　(b) Roughness by core barrel

Fig. 8. Roughness profiles at DT site

core barrel [Figure 6 (a)], and (2) discontinuous drilling processing of the core barrel due to rock coring produced a rougher borehole.

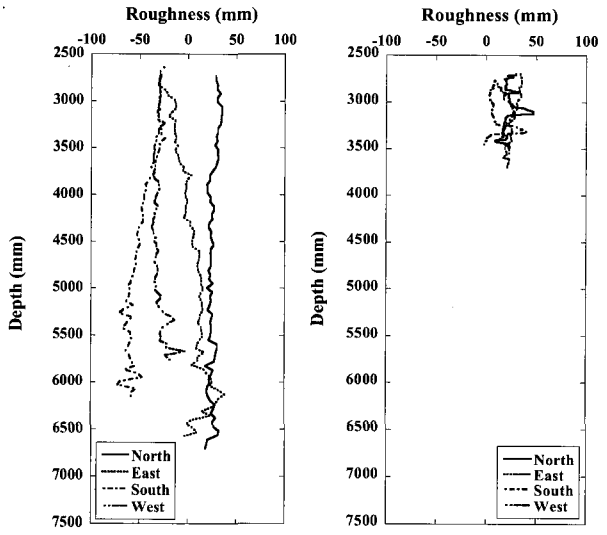

(a) Roughness by auger (b) Roughness by core barrel

Fig. 9. Roughness profiles at RC site

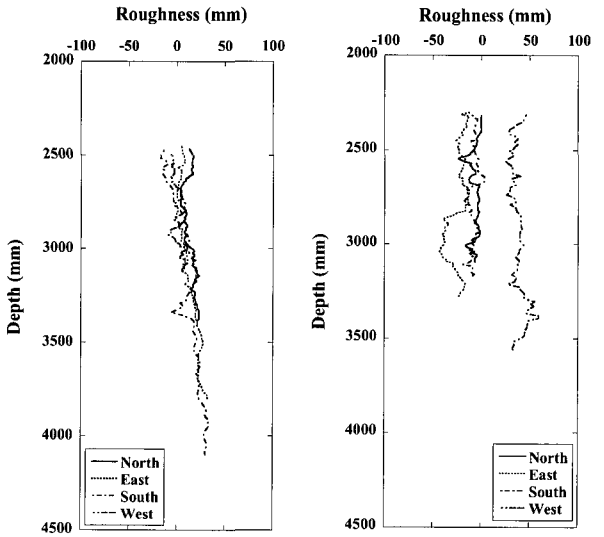

(a) Roughness by auger (b) Roughness by core barrel

Fig. 10. Roughness profiles at TS site

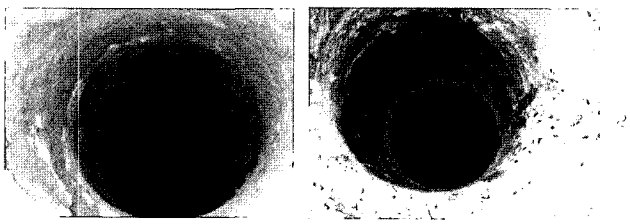

(a) Auger Test Hole (b) Core Barrel Test Hole

Fig. 11. Photos of boreholes excavated by auger and core barrel at TS site

5. Analysis of Socket Roughness

5.1 Roughness-Length Method

The roughness-length method (RLM), a simple procedure for estimating the fractal dimension of self-affine series and proposed by Malinverno (1990), was applied to analyze the socket roughness statistics in this study. Using the concepts adopted from fractal geometry of self-affine series, it was possible to analyze these roughness profiles using the RLM to obtain roughness statistics such as mean roughness and standard deviation of the roughness. For a self-affine fractal profile, the window length w (as shown in Figure 12) was used to relate to the standard deviation of the roughness profile height as follows,

$$s(r) = Aw^H, \tag{3}$$

where $s(r)$ = standard deviation of the roughness profile height,

w = spanning length of the profile,

H = Hurst exponent can be estimated from the slope of the plot between logarithm of $s(r)$ and logarithm of w and,

A = proportionality constant also can be estimated from the intercept of the plot between logarithm of $s(r)$ and logarithm of w.

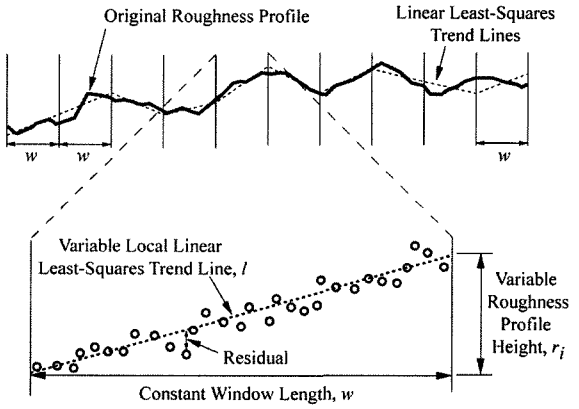

Mean Roughness Height $= \bar{r} = \frac{1}{n_w}\sum_{i=1}^{n_w}|r_i| = \Delta r$

Standard Deviation of $r = s(r) = RMS(r) = \frac{1}{n_w}\sum_{i=1}^{n_w}\sqrt{\frac{1}{m_i - 2}\sum_{j\in w_i}(z_j - \bar{z})}$

Fig. 12. Main characteristics of the RLM (after Kulatilake and Um, 1999)

Malinverno (1990) proposed the relation between $s(r)$ and w, the $s(r)$ (using RLM) calculated as the root-mean-square (RMS) value of the profile height residuals on a linear least-squares trend line fitted to the sample points in a window of length, w, as shown in Figure 12 according the following equation

$$s(r) = RMS(r) = \frac{1}{n_w}\sum_{i=1}^{n_w}\sqrt{\frac{1}{m_i - 2}\sum_{j\in w_i}(z_j - \bar{z})^2}, \quad (4)$$

where n_w = total number of windows of length w,
m_i = number of points in window w_i,
z_j = residuals on the trend and,
$\bar{z}$ = mean residual in window w_i.

Based on Figure 12, mean of absolute roughness height, $\bar{r} = \Delta r$ was also calculated as below,

$$\bar{r} = \frac{1}{n_w}\sum_{i=1}^{n_w}|r_i| = \Delta r, \quad (5)$$

This process was carried out using the Microsoft Excel spread sheets to analyze roughness profile by traversing the profile with the constant window length, w. This process was performed for various constant window lengths (10 to 80 mm with 10 mm intervals) up to approximately 10% of the socket diameter (76.2 mm ≈ 80 mm) as suggested by Seidel (2000).

5.2 Socket Roughness Analysis by RLM

The results of roughness analysis are shown in Figures 13 through 16. As described in the previous section, mean borehole roughness height due to the core barrel was higher than the auger drilling. For the HT site as shown in Figure 13, the mean roughness height of the core barrel test hole was approximately 40% higher than the auger test hole for the various constant window lengths. Also, the standard deviation of the roughness profile height of the core barrel test hole was approximately 30% higher than the auger test hole along with various constant window lengths.

For the DT site as shown in Figure 14, the mean roughness height of the core barrel test hole was approximately 10% higher than the auger test hole along with the various constant window lengths. Also, the standard deviation of the roughness profile height of the core barrel test hole was approximately the same as the auger test hole along various window lengths.

For the RC site as shown in Figure 15, the mean roughness height of the core barrel test hole was approximately 20% higher at the window length of 10 mm than the auger test hole, and then gradually increased up to 70% at the window length of 80 mm. The standard deviation of the roughness profile height of the core barrel was approximately 40% less at the window length

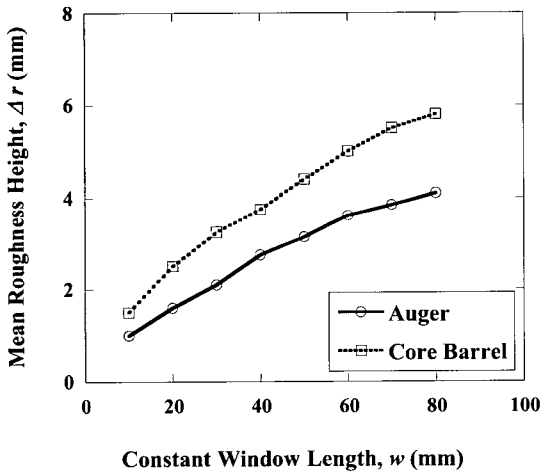

(a) Δr versus w

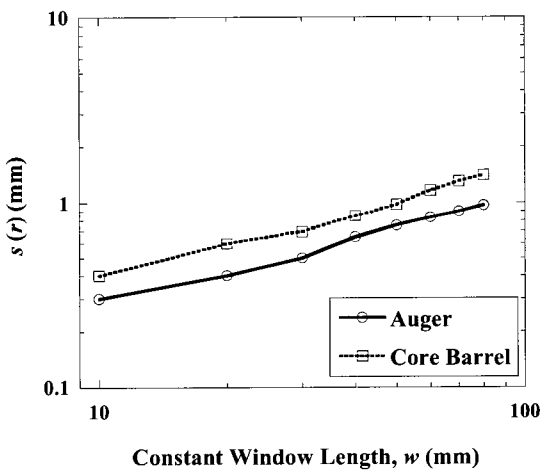

(b) $s(r)$ versus w

Fig. 13. RLM analysis results for the HT site

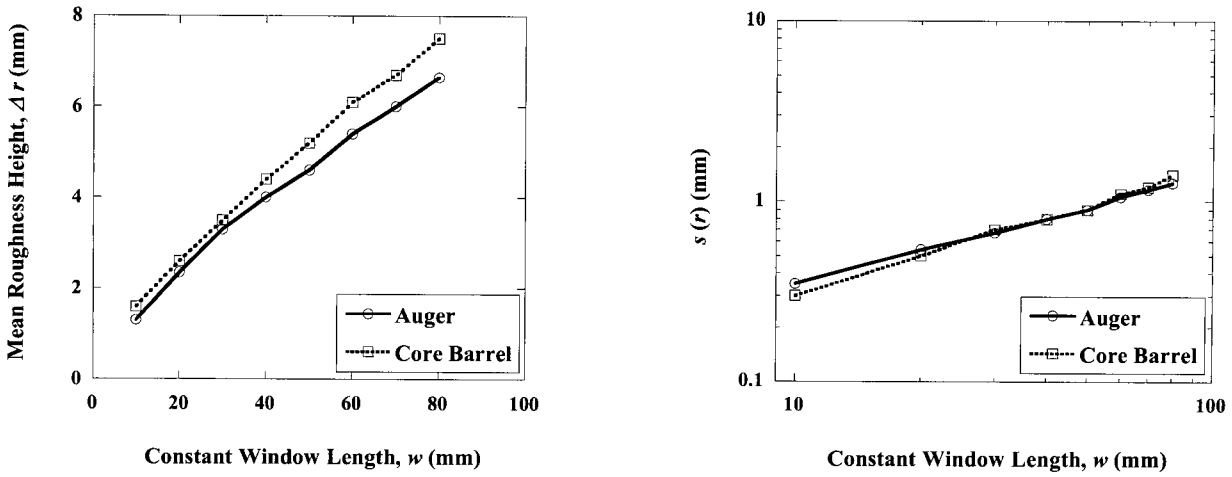

(a) Δr versus w (b) $s(r)$ versus w

Fig. 14. RLM analysis results for the DT site

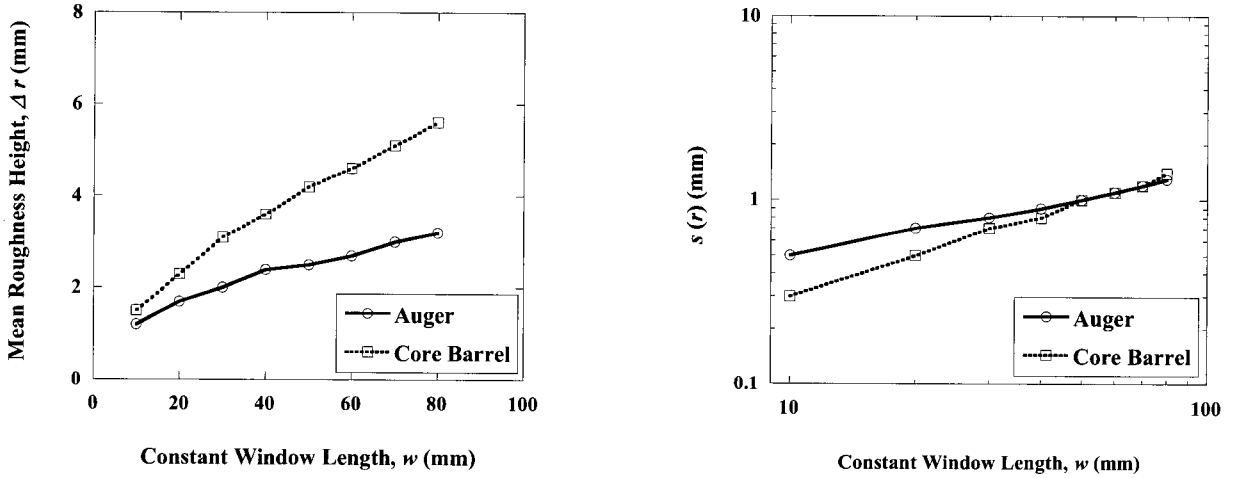

(a) Δr versus w (b) $s(r)$ versus w

Fig. 15. RLM analysis results for the RC site

of 10 mm than auger drill which reduced with increased window length.

For the TS site as shown in Figure 16, the mean roughness height of the core barrel was approximately 20% higher than the auger drill. Also, the standard deviation of the roughness profile height produced by the core barrel was approximately 30% higher than the auger drill.

The results of socket roughness analysis using the RLM for all test sites are summarized in Table 1. Based on Table 1, it was evident that the roughness of the borehole was affected by the drilling tools. The roughness caused by the core barrel was about 30% rougher than the auger drill in overall. However, the socket roughness was not much related with rock types (clay shale and limestone) and their unconfined compressive strengths.

Average socket roughness values in the Table 1 were compared with the back-calculated values of effective roughness height proposed by Seidel and Collingwood (2001) (Figure 1), and the result of the comparison is shown in Figure 17. It was noted that the unconfined compressive strength (q_u) for TS site was assumed as 8 MPa in Figure 17. The socket roughness in this study was close to the lower limit proposed by Seidel and Collingwood (2001), and had similar trend with their lower limit.

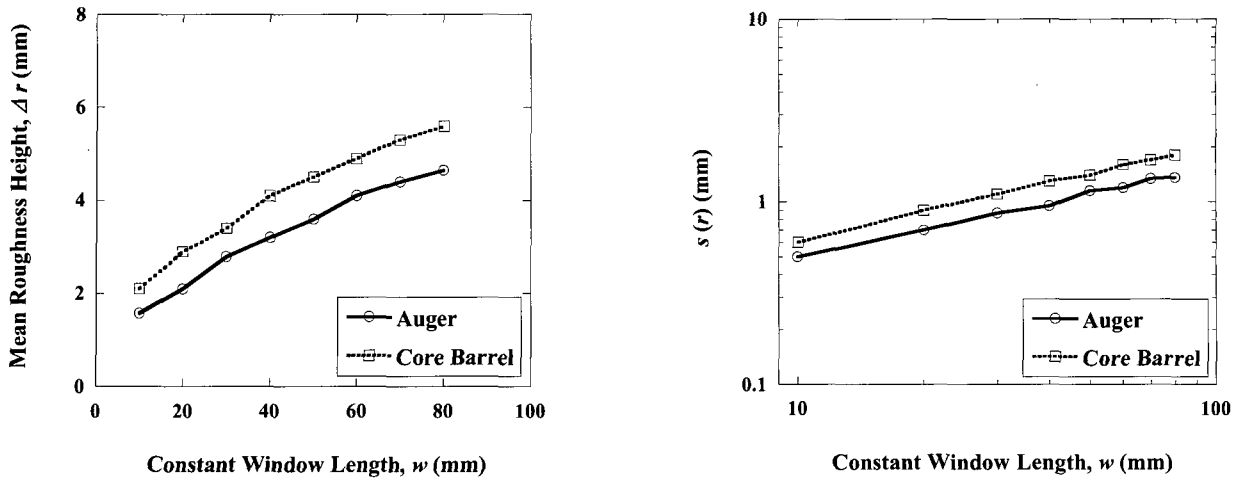

(a) Δr versus w (b) $s(r)$ versus w

Fig. 16. RLM analysis results for the TS site

Table 1. Socket roughness heights (Δr) based on cord lengths (w)

Sites	Rock Type / q_u	Types of Drilling*	Δr for corresponding w (mm)				Average Values	Overall $\Delta r_C/\Delta r_A$
			w = 10	w = 30	w = 50	w = 70		
HT	Clay Shale / 1.2 (MPa)	Δr_A	1.0	2.1	3.2	3.8	2.5	1.3
		Δr_C	1.5	3.3	4.4	5.5	3.7	
		Δr_C / Δr_A	1.4	1.6	1.4	1.5	1.5	
DT	Clay Shale / 2.1 (MPa)	Δr_A	1.4	3.3	4.7	6.0	3.8	
		Δr_C	1.5	3.5	5.2	6.7	4.2	
		Δr_C / Δr_A	1.1	1.1	1.1	1.1	1.1	
RC	Limestone / 10.0 (MPa)	Δr_A	1.2	2.0	2.5	3.1	2.2	
		Δr_C	1.5	3.1	4.2	5.1	3.5	
		Δr_C / Δr_A	1.2	1.5	1.7	1.7	1.5	
TS	Limestone / N/A	Δr_A	1.6	2.8	3.6	4.4	3.1	
		Δr_C	2.1	3.4	4.5	5.3	3.8	
		Δr_C / Δr_A	1.3	1.2	1.3	1.2	1.3	

*Δr_A is roughness by Auger and Δr_C is roughness by core barrel.

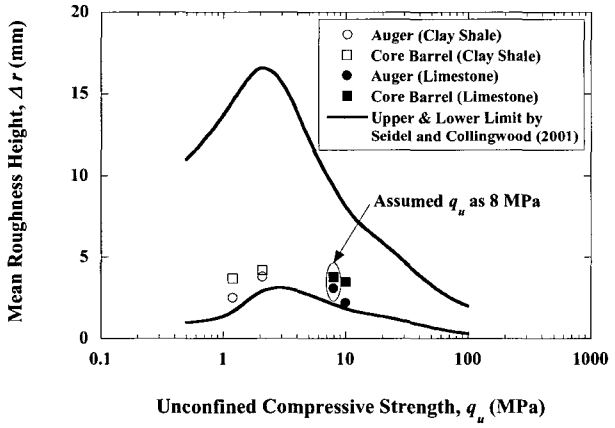

Fig. 17. Comparison of roughness height with upper and lower limits proposed by Seidel and Collingwood (2001).

6. Conclusions

Based on this study, the following conclusions are drawn;

(1) A laser borehole roughness profile device (LBRP) was developed in this study using the laser triangulation principle to measure the roughness.

(2) Two different types of drilling tools (auger and core barrel) were applied to the four test sites, and LBRP was used to measure the socket roughness.

(3) The socket roughness developed by the core barrel

was about 30% rougher than that by the auger in overall.

(4) The socket roughness was affected with the types of drilling tools. However, the socket roughness was not related with rock types and also their unconfined compressive strengths.

References

1. Seidel, J. P. and Collingwood, B. (2001), "A New Socket Roughness Factor for Prediction of Rock Socket Shaft Resistance", *Canadian Geotechnical Journal*, Vol.38, February, pp.138-153.
2. Horvath, R. G., Kenney, T. C. and Kozicki, P. (1983), "Methods of Improving the Performance of Drilled Piers in Weak Rock", *Canadian Geotechnical Journal*, Vol.20, pp.758-772.
3. Kulatilake, P. H. S. W. and Um, J. (1999), "Requirements for Accurate Quantification of Self-Affine Roughness Using the Roughness-Length Method", *International Journal of Rock Mechanics and Mining Sciences*, Vol.36, pp.5-18.
4. Kulhawy, F. H. and Phoon, K-K (1993), "Drilled Shaft Side Resistance in Clay Soil to Rock", *Design and Performance of Deep Foundations, GSP No. 38*, Ed. by P. P. Nelson, T. D. Smith and E. C. Clukey, ASCE, October, pp.172-183.
5. Liang, R. (2002), *Development of A Laser Triangulation Distance Measurement Device and Its Application to Borehole Roughness Detection*, MSEE Thesis, Department of Electrical Engineering, University of Houston, Houston, Texas.
6. Malinverno, A. (1990), "A Simple Method to Estimate The Fractal Dimension of A Self Affine Series", *Geophysical Research Letters*, Vol.17, pp.1953-1956.
7. Rowe, P. K. and Armitage, H. H. (1987), "A Design Method for Drilled Piers in Weak Rock", *Canadian Geotechnical Journal*, Vol.24, pp.126-142.
8. O'Neill, M. W. and Hassan, K. M. (1993), "Perimeter Load Transfer in Drilled Shafts in the Eagle Ford Formation", *GSP No. 38*, Ed. by P. P. Nelson, T. D. Smith and E. C. Clukey, ASCE, October, pp.229-244.
9. Seidel, J. P. (2000), *ROCKET Executable File*, Department of Civil Engineering, Monash University, Melbourne, Victoria, Australia.

(접수일자 2006. 6. 7, 심사완료일 2006. 9. 21)